Room temperature photon avalanche upconversion in Tm^{3+}-doped fluoroindate glasses

2000 J. Phys.: Condens. Matter 12 1507

(http://iopscience.iop.org/0953-8984/12/7/331)

J. Phys.: Condens. Matter **12** (2000) 1507–1516. Printed in the UK PII: S0953-8984(00)06928-9

Room temperature photon avalanche upconversion in Tm^{3+}-doped fluoroindate glasses

I R Martín†, V D Rodríguez†, Y Guyot‡, S Guy‡, G Boulon‡ and M-F Joubert‡

† Departamento Física Fundamental y Experimental, Universidad de La Laguna, 38206 La Laguna, Tenerife, Spain
‡ Laboratoire de Physico-Chimie des Matériaux Luminescents, UMR CNRS No 5620, Université de Lyon 1, 43 boulevard 11 Novembre 1918, 69622 Villeurbanne Cédex, France

Received 13 August 1999 , in final form 3 November 1999

Abstract. Intense blue upconversion emission has been observed at room temperature under excitation in the range of 630–660 nm in a fluoroindate glass doped with 2.5 mol% of Tm^{3+}. The experimental dynamics and power dependence of this emission are well described using a photon avalanche model based on the mean field approximation.

1. Introduction

There is currently a great interest in converting near infrared laser diode light into visible light using upconversion processes. These processes involve stepwise excitation and/or energy transfers between ions. They can be efficient in rare earth doped materials and, sometimes, give rise to upconversion laser effects (see tables 3 and 4 in [1]). Photon avalanche is one of these upconversion processes which was first discovered in Pr^{3+}-based infrared quantum counters [2, 3] and which has two main characteristics [4]. The first one is that the pump photon energy is only resonant between a metastable state and a higher level of the active ions. The second one is an excitation power threshold which corresponds to a sudden absorption of the pump photons and, therefore, to a sudden increase of the upconverted fluorescence; at the same time, there is a slowing down and a change of the rise shapes of the transient signals.

Fluoroindate glasses are promising materials for photonic applications due to their large transparency (from 250 nm to 9 μm) and low multiphonon relaxation rates due to the low phonon energies obtained in these glasses (about 500 cm^{-1}). Therefore, efficient upconversion emissions have been obtained with different rare earth ions as dopants in fluoroindate glasses [5–8]. We observed photon avalanche red to blue upconversion in such glasses doped with Tm^{3+} ions and this is the subject of this work.

In the next section, we shall present a brief summary of the theoretical photon avalanche model, then describe the material and the experimental equipment necessary to evaluate all the necessary spectroscopic parameters and to observe the photon avalanche effect. Finally, the experimental results will be presented and discussed and, in the conclusions, the photon avalanche behaviour presented here will be compared to that observed in other Tm^{3+}-doped compounds.

0953-8984/00/071507+10$30.00

2. Photon avalanche rate equation system

The photon avalanche process leading to the strong blue emission ($^1G_4 \rightarrow {}^3H_6$) of Tm^{3+} ions after red excitation resonant with the $^3F_4 \rightarrow {}^1G_4$ transition has been studied in different materials [1]. The microscopic description of this process is schematized in figure 1. As all ions are initially in the ground state 1 (no thermal population of level 2), the effect of the pump is minimal. If one ion is promoted to the metastable state 2, whatever the mechanism of population of this state, it may be further excited to level 4 by absorption of the pump photon. Then, if the concentration of Tm^{3+} is high enough, the cross relaxation energy transfer given by the s_4 and s_3 channels (see figure 1) promote the excited ion and two of its neighbours into the metastable level $^3F_4$, after which these three ions newly can be excited into the $^1G_4$ level and so on. This gives rise to efficient emission from the $^1G_4$ level at about 475 nm and the dynamics of this process can be described by the following rate equations [4]

$$dn_4/dt = R_2 n_2 - W_4 n_4 - s_4 n_1 n_4 \tag{1}$$

$$dn_3/dt = R_1 n_1 - (W_3 + W_3^{NR}) n_3 + b_{43} W_4 n_4 + s_4 n_1 n_4 - s_3 n_3 n_1 + Q_{23} n_2^2 \tag{2}$$

$$dn_2/dt = -(R_2 + W_2) n_2 + b_{42} W_4 n_4 + (b_{32} W_3 + W_3^{NR}) n_3 + s_4 n_1 n_4 + 2 s_3 n_1 n_3 - (Q_{22} + 2Q_{23}) n_2^2 \tag{3}$$

$$n_1 + n_2 + n_3 + n_4 = 1. \tag{4}$$

In these equations R_1 and R_2 correspond to the ground and $^3F_4$ excited state pumping rates, W_i is the single ion radiative relaxation rate of the level i, W_3^{NR} is the multiphonon relaxation rate from level 3, b_{ij} is the branching ratio from level i to level j and the s_3 and s_4 parameters are the cross relaxation energy transfer rates. Finally, at high excitation power, upconversion processes from the $^3F_4$ metastable level are possible and they are described by Q_{ij} parameters, i.e.

$$Q_{23} : {}^3F_4 + {}^3F_4 \rightarrow {}^3H_6 + {}^3H_4 \tag{5}$$

$$Q_{22} : {}^3F_4 + {}^3F_4 \rightarrow {}^3H_6 + {}^3H_5. \tag{6}$$

So, in addition to photon avalanche upconversion experiments under red cw excitation, we shall record absorption spectra and fluorescence decays to evaluate most of these parameters. Them we shall confront this theory with the photon avalanche experimental results.

In avalanche upconversion experiments emission at 445 nm coming from the $^1D_2$ level is also observed. This level may be excited by different mechanisms depending on the power pump which will be analysed below.

3. Experiment

The fluoroindate glasses were prepared at Departamento de Física de La Materia Condensada (University of Zaragoza, Spain). The starting composition for sample preparation was in mol%: $(40 - x)\mathrm{Ln}\,F_3$, $20ZnF_2$, $20SrF_2$, $20BaF_2$, $x TmF_3$, with x equal to 0.1 or 2.5. All compounds used were of 99.5% purity or better. The mixture of the desired composition was heated for one hour at 400 °C with $NH_4F.HF$ in order to force the conversion of residual oxide species to fluorides. After this process the mixture was melted at 900 °C. Finally, the melt was poured into an aluminium mould preheated to 250 °C, yielding glass plates of 1–2 mm thick. The refractive index obtained in these glasses is 1.5.

All the spectroscopic measurements were made at room temperature and using the experimental equipment described in this section.

Absorption spectra were performed using a Perkin Elmer Lambda 9 spectrophotometer.

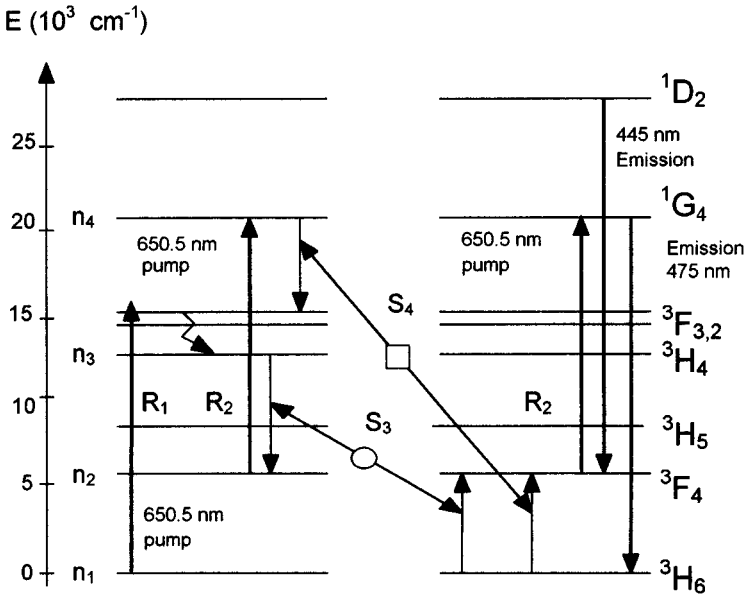

Figure 1. Energy level diagram of Tm^{3+} ions in fluoroindate glasses. The avalanche process is indicated.

Selective excitation in the $^1G_4$ manifold was performed using an excimer laser (pulse length: 10 ns, variable repetition rate and energy per pulse up to 50 mJ at 308 nm) followed by one-amplifier-stage dye laser (pulse length: 10 ns and line width: 0.1 cm^{-1}) containing a Coumarin 480 solution. Selective excitation in the $^3F_2$ state was performed using a frequency doubled Nd:YAG laser (pulse length: 10 ns, repetition rate: 10 Hz and energy per pulse up to 300 mJ at 532 nm) followed by a three-amplifier-stage dye laser (pulse length: 10 ns and line width: 0.1 cm^{-1}) containing a DCM solution. The emissions from the $^1G_4$ and from the $^3H_4$ levels were then analysed by a 1 m Hilger and Watts monochromator with a dispersion of 0.8 nm mm^{-1} and detected by an RCA GaAs photomultiplier tube. The signal was processed by an Ortec photon counting system. The fluorescence decay time measurements were realized using a Canberra 35+ multichannel analyser with a maximum resolution of 200 ns per channel.

The saturation rate of the $^3F_4$ metastable by analysing the $^3F_4$ fluorescence decay versus the excitation density. Selective excitation in $^3F_4$ was performed with the frequency doubled Nd:YAG pumped dye laser containing pyridine 1 solution and followed by a Raman cell. The excitation intensity was varied using neutral density filters and the Guassian beam was focused in the sample with a 500 mm focal lens. The waist spot size on the sample (defined as the $1/e^2$ radius of the intensity) was shown to be 37×37 μm^2. The emission was analysed with a 1/4 m Jobin–Yvon monochromator with a dispersion of 6 nm mm^{-1} followed by an AsIn detector. The signal was acquired by a Lecroy 9410 digital oscilloscope controlled by a personal computer.

For photon-avalanche-pumped upconverted fluorescence, laser excitation was achieved by a continuous wave Ar^+-laser-pumped ring dye laser with Kiton Red solution. The laser beam was chopped and focused on the sample with a 50 mm focal length lens. The waist spot size in the sample was shown to be 9×9 μm^2. The anti-Stokes fluorescence was collected at right angles to the laser beam direction and was analysed by a 1/4 m Jarrel–Ash monochromator followed by an EMI 9789QB photomultiplier. The signal was acquired by a Lecroy 9410

digital oscilloscope for dynamics study or by a digital–analogue card for spectral study. All this experimental set-up was controlled by a personal computer.

4. Results and discussion

4.1. De-excitation rates

From the absorption spectrum of the fluoroindate glass doped with 2.5 mol% of Tm^{3+} the experimental oscillator strengths for transitions from the ground state to the different excited states have been obtained. The Judd–Ofelt parameters [9, 10] obtained from these experimental oscillator strengths are $\Omega_2 = 1.9 \times 10^{-20}$, $\Omega_4 = 1.7 \times 10^{-20}$ and $\Omega_6 = 1.1 \times 10^{-20}$ cm^2. These values are similar to those ones found in the literature for Tm^{3+} ions in other matrices [11–16].

The spontaneous emission probabilities for the emitting levels of interest in this work have been calculated using the Judd–Ofelt parameters; the results are presented in table 1. From these values the branching ratios b_{ij} of the transitions which will be involved in the photon avalanche process have been obtained and are listed in table 2.

Table 1. Calculated electric and magnetic dipole contributions to the spontaneous emission probabilities in fluoroindate glasses doped with Tm^{3+}.

Transition	λ (nm)	A_{ED} (ms^{-1})	A_{MD} (ms^{-1})
$^3F_4 \rightarrow {}^3H_6$	1800	0.107	
$^3H_4 \rightarrow {}^3H_5$	2330	0.018	0.005
$^3F_4$	1460	0.055	0.012
$^3H_6$	801	0.572	
$^1G_4 \rightarrow {}^3F_2$	1557	0.011	
$^3F_3$	1437	0.037	0.002
$^3H_4$	1112	0.126	0.021
$^3H_5$	777	0.372	0.073
$^3F_4$	649.5	0.097	0.007
$^3H_6$	479	0.472	
$^1D_2 \rightarrow {}^1G_4$	1575	0.072	
$^3F_2$	780.5	0.578	0.033
$^3F_3$	747.5	0.449	0.054
$^3H_4$	660	0.781	
$^3H_5$	512	0.068	
$^3F_4$	452	6.075	
$^3H_6$	362.5	5.667	

The multiphonon relaxation rate W_3^{NR} can be estimated using the gap law, i.e.

$$W^{NR} = W^{NR}(0)\exp(-\alpha\Delta E) \tag{7}$$

where $W^{NR}(0)$ and α are positive constants characteristics of the host and ΔE is the gap difference. In fluoroindate glasses the values obtained for $W^{NR}(0)$ and α are 1.0×10^7 m s^{-1} and 5.7×10^{-3} cm, respectively [17]. Assuming a gap difference between the $^3H_4$ and $^3H_5$ levels of 4430 cm^{-1} a negligible multiphonon probability for the $^3H_4$ level is estimated. This result can be explained on the basis of the low phonon energy obtained in these glasses (about 500 cm^{-1}) with respect to the gap difference, so about nine phonons are necessary to produce multiphonon de-excitation.

Table 2. Spectroscopic parameters obtained at room temperature in fluoroindate glasses doped with Tm^{3+}.

W_2 (ms^{-1})	0.270	measured in the 2.5% doped glass under low excitation power
W_3 (ms^{-1})	0.526	measured in low doping glass [21]
W_3^{NR} (ms^{-1})	0	estimated by gap law
W_4^{NR} (ms^{-1})	1.370	measured in low doping glass [21]
b_{ij}	$b_{32} = 0.136$	
	$b_{42} = 0.451$	
	$b_{43} = 0.162$	
η_i	$\eta_3 = 0.967$	
	$\eta_4 = 0.966$	
S_i	s_3 (ms^{-1}) $= 15.7$	
	S_4 (ms^{-1}) $= 39.0$	
Q_{23} (ms^{-1})	0.07	

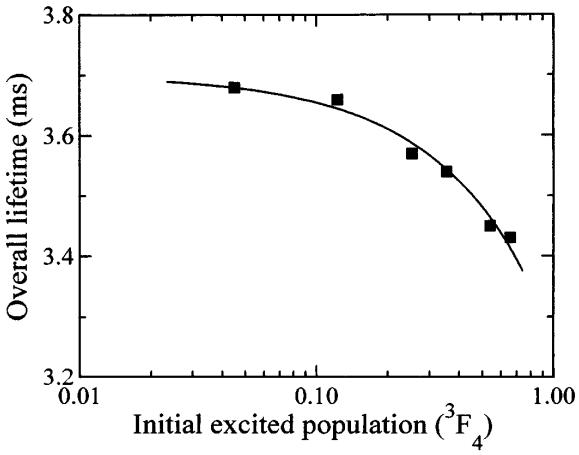

Figure 2. Variation of the overall lifetime with the initial $^3F_4$ population for a fluoroindate glass doped with 2.5 mol% of Tm^{3+} (■). The solid line is the fit to the theoretical expression obtained from the rate equation taking into account the Gaussian excitation beam profile.

4.2. Cross relaxation energy transfer rates

The quantum yield of the cross relaxation mechanism corresponding to a level with a lifetime τ_i can be derived from the fluorescence decays using the following equation,

$$\eta_i = 1 - \frac{1}{\tau_i I(0)} \int_0^\infty I(t)\,\mathrm{d}t = \frac{s_i}{\tau_i^{-1} + s_i} \tag{8}$$

where $I(t)$ is the emitted fluorescence intensity and s_i is the cross relaxation rate of the level i. The luminescence decays for Tm^{3+} ions have been measured after pulsed excitation into the $^1G_4$ and $^3H_4$ levels and the cross relaxation rates, respectively s_4 and s_3, have been calculated using equation (8). The values obtained with the 2.5 mol% Tm^{3+} doped glass are presented in table 2 together with the probabilities W_4 and W_3 measured in a glass with 0.1 mol% Tm^{3+} concentration, in which the cross relaxation processes are negligible [18].

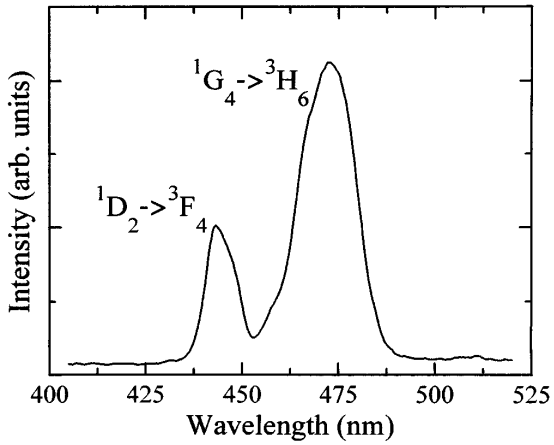

Figure 3. Upconversion emission spectrum obtained in a fluoroindate glass doped with 2.5 mol% of Tm^{3+} by exciting at 650.5 nm with an excitation power of 100 mW.

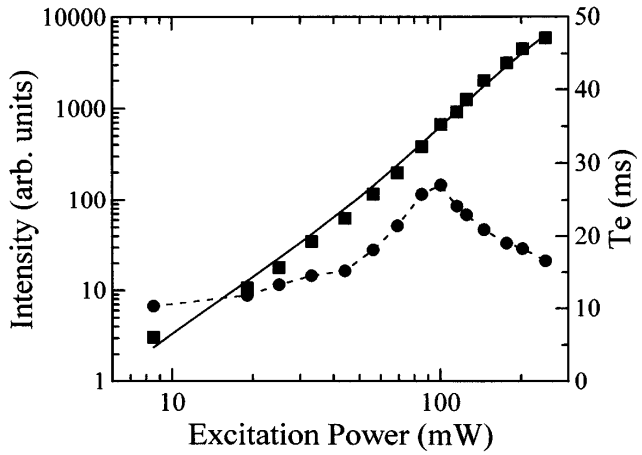

Figure 4. Dependence on the excitation power of the upconversion emission intensity (■) and the time of establishment T_e (● −− ●) obtained in a fluoroindate glass doped with 2.5 mol% of Tm^{3+} by exciting at 650.0 nm and detecting at 475 nm. The solid line is the theoretical dependence of the emission at 475 nm obtained from the rate equations (1)–(4) for stationary excitation taking into account the Gaussian excitation beam profile.

4.3. Upconversion rate from the $^3F_4$ level

Under pulsed laser excitation into the $^3F_4$ level in the fluoroindate glass doped with 2.5 mol% of Tm^{3+}, luminescence corresponding to the $^3H_4 \rightarrow {}^3H_6$ transition can be observed. This upconversion process can be explained on the basis of the channel given by (5). At low excitation power, the decay curves corresponding to the $^3F_4 \rightarrow {}^3H_6$ transition have exponential character. However, when the excitation power is increased, an increasing nonexponentiality is observed. In these decay curves, the overall lifetimes has been obtained using the expression

$$\langle \tau \rangle = \frac{1}{I(0)} \int_0^\infty I(t)\,\mathrm{d}t \tag{9}$$

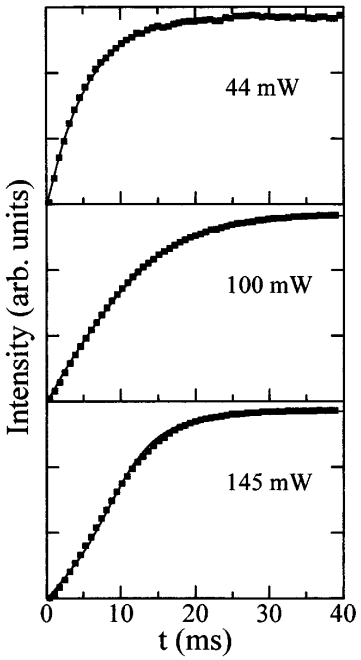

Figure 5. Experimental rise of the 475 nm upconversion emission (■) obtained with different excitation power at 650.5 nm in a fluoroindate glass doped with 2.5 mol% of Tm^{3+}. The solid lines correspond to the fits to the rate equations (1)–(4) taking into account the Gaussian excitation beam profile.

where $I(t)$ is the fluorescence intensity corresponding to the $^3F_4 \rightarrow {}^3H_6$ transition. Figure 2 shows these experimental overall lifetimes.

The upconversion rates of this process can be obtained by analysing the $^3F_4$ fluorescence decay versus the initial population of this level. This procedure has been used previously to get the upconversion rates in Nd^{3+}-doped YAG crystals [9]. The rate equation that describes the $^3F_4$ population of Tm^{3+} ions, after direct pulsed excitation into this level, is given by

$$\frac{dn_2}{dt} = -W_2 n_2 - (Q_{22} + 2Q_{23})n_2^2 \tag{10}$$

and the solution to this equation is

$$n_2(t) = \frac{n_2(0)\exp(-W_2 t)}{1 + n_2(0)(Q_{22} + 2Q_{23})[1 - \exp(-W_2 t)]}. \tag{11}$$

The overall lifetime for this level, taking into account a Gaussian profile excitation, can be expressed as

$$\langle \tau \rangle = \left[\int_0^\infty \left(\int_0^\infty n_2(t, r) 2\pi r \, dr \right) dt \right] \left(\int_0^\infty n_2(0, r) 2\pi r \, dr \right)^{-1}. \tag{12}$$

The experimental overall lifetimes shown in figure 2 have been fitted to equation (12). From this fit a low value of 0.07 ms^{-1} has been obtained for $Q_{22} + 2Q_{23}$. Moreover, due to the energy gap differences in the respective upconversion processes (about 390 and 2800 cm^{-1} for Q_{23} and Q_{22}, respectively), it is expected that $Q_{23} \gg Q_{22}$.

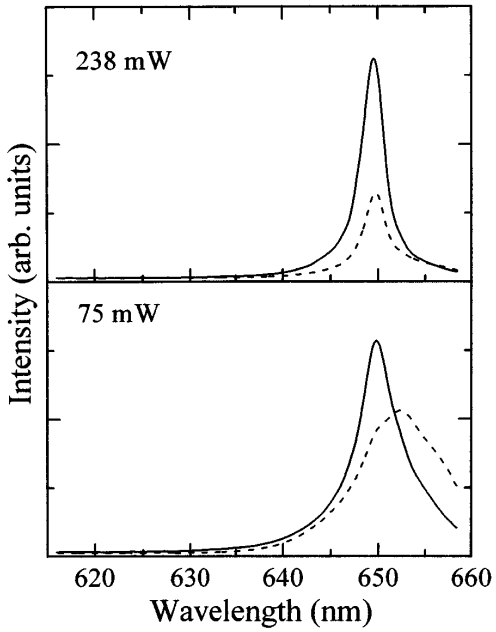

Figure 6. Excitation spectra of the two emission bands centred at 475 nm (——) and 445 nm (– – –) under low (75 mW) and high (238 mW) excitation power obtained in a fluoroindate glass doped with 2.5 mol% of Tm^{3+}.

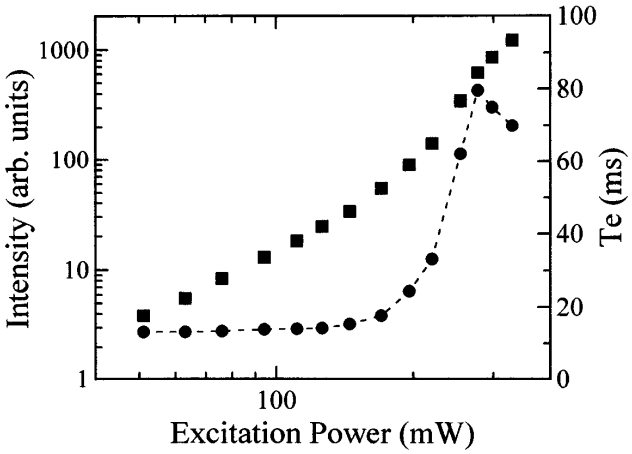

Figure 7. Dependence on the excitation power of the upconversion emission intensity (■) and the time of establishment Te (● – – ●) obtained in a fluoroindate glass doped with 2.5 mol% of Tm^{3+} by exciting at 630.4 nm and detecting at 475 nm.

4.4. Photon avalanche upconversion

The blue upconversion emission observed in the 2.5 mol% Tm^{3+} doped fluoroindate glass by exciting with the cw dye laser at 650.5 nm is presented in figure 3. The two bands can be assigned to $^1D_2 \rightarrow {}^3F_4$ and $^1G_4 \rightarrow {}^3H_6$ transitions around 445 and 475 nm, respectively. The dependence of the blue emission intensity at 475 nm under stationary conditions on the excitation power is shown in figure 4. At low excitation density, a quadratic dependence is

observed, but around 100 mW a sudden increase of the blue emission occurs. The time of establishment T_e, defined as the time necessary to reach 95% of the blue stationary intensity is also included in figure 4. At about 100 mW, T_e presents a maximum and the rise curves change their shape (see figure 5). These results are indicative of a photon avalanche effect with an apparent excitation power threshold I_{2th} of 100 mW. The emission band centred at 445 nm shows a quite different behaviour. Its stationary intensity shows an almost instantaneous build-up at very low excitation power, then images the 475 nm fluorescence rise time at high power. This is explained by the fact that two step absorption ($^3H_6 \rightarrow {}^3F_2$ then $^3H_4 \rightarrow {}^1D_2$) is used to feed the $^1D_2$ state at low power while the energy transfer process which involves the $^1G_4$ level ($^1G_4, ^3H_4 \rightarrow {}^1D_2, ^3F_4$ or $^1G_4, ^3F_4 \rightarrow {}^1D_2, ^3H_6$) causes the long build-up observed in the high power regime. This interpretation is validated by the excitation spectra of $^1D_2 \rightarrow {}^3F_4$ and $^1G_4 \rightarrow {}^3H_6$ emissions presented in figure 6: for low excitation power, the excitation band of the $^1G_4 \rightarrow {}^3H_6$ emission is centred at 649.5 nm while the excitation band of the $^1D_2 \rightarrow {}^3F_4$ emission is centred at 652.5 nm; but for excitation power well above the avalanche threshold the two excitation bands are similar and centred at 649.5 nm.

The experimental transient curves presented in figure 5 have been fitted to the evolution of the n_4 population predicted by the differential rate equations (1)–(4) and taking into account the Gaussian profile of the laser beam [4]. The parameters presented in table 2 have been used in the fits. So, except the pumping rates R_1 and R_2, all the spectroscopic parameters are known and fixed. As can be seen in figure 5 a good fit is obtained using the cross sections $\sigma_1^{650.5} = R_1/I = 1.39 \times 10^{-22}$ cm^{-22} cm^2 and $\sigma_2^{650.5} = R_2/I = 5.35 \times 10^{-22}$ cm^2. Moreover with these values has been obtained the theoretical excitation power dependence of the stationary blue intensity presented in figure 4. From the absorption spectrum a value of 1.30×10^{-22} cm^2 has been obtained for $\sigma_1^{650.5}$, which is in good agreement with the previous value obtained from the photon avalanche fits.

The avalanche effect for the upconversion blue emission at 475 nm when the excitation is carried out at wavelength shorter than 650.5 nm also is observed but the experimental power threshold increases. Figure 7 shows the results obtained with an excitation wavelength of 630.4 nm. It appears that $I_{2th} = 277$ mW; moreover, T_e increases also as it is equal to 80 ms compared to 27 ms in the previous case. This behaviour is probably an effect of the absorption cross sections σ_1 and σ_2 for the two excitation wavelengths. To evaluate $\sigma_1^{630.4}$ and $\sigma_2^{630.4}$, we fitted the photon avalanche curves and obtained 6.93×10^{-24} cm^2 and 1.86×10^{-22} cm^2, respectively. It is then easy to check that, as predicted by the theory [4], I_{2th} is inversely proportional to σ_2 and T_e is proportional to the square root of σ_2/σ_1.

Finally, we comment that the relatively high emission from the $^1D_2$ level in figure 3 suggests that this level must be taken into account in the rate equations. Although a more complete description of the process would be obtained in this way, on the other hand the number of unknown parameters in the fits would be excessive, due to the different mechanisms of excitation and de-excitation of the $^1D_2$ level. Additionally, the good agreement with the experimental results obtained using the rate equations (1)–(4) indicates that these equations describe reasonably well the avalanche process. The $^1D_2$ emission is a loss mechanism for the $^1G_4$ emission in these experiments but we must take into account the interesting possibility of obtaining emission at 445 and also at 360 nm (with similar intensities from data in table 1) with relatively high efficiency from the $^1D_2$ level in these glasses.

5. Conclusions

We have observed intense blue emission when pumping in the 630–660 nm range at room temperature in a fluoroindate glass doped with 2.5 mol% Tm^{3+}. Experimental results are

well described using the photon avalanche rate equation model in which all the spectroscopic parameters involved have been determined experimentally. It appears that in such red to blue photon avalanche upconversion in a Tm^{3+}-doped glass, as was also observed in the case of Tm^{3+}-doped BIGaZYTZr glasses [16], the threshold is not very spectacular because glasses have broad absorption lines implying a significant overlap between ground state absorption and the $^3F_4 \rightarrow {}^1G_4$ excited state absorption. This was also the case with the red to blue photon avalanche upconversion studied in Tm^{3+}-doped Y_2O_3 crystals [20] in which the σ_1/σ_2 ratio is much higher than measured in Tm^{3+}-doped YAP or YAG crystals [21].

Acknowledgments

We would like to thank Professor R Alcalá for supplying the samples studied in this work, which was partially supported by 'Gobierno Autónomo de Canarias'.

References

[1] Joubert M-F 1999 *Opt. Mater.* **11** 181
[2] Chivian J S, Case W E and Eden D D 1979 *Appl. Phys. Lett.* **35** 124
[3] Kueny A W, Case W E and Koch M E 1989 *J. Opt. Soc. Am.* B **6** 639
[4] Guy S, Joubert M-F and Jacquier B 1997 *Phys. Rev.* B **55** 8240
[5] Catunda T, Nunes L A O, Florez A, Messaddeq Y and Aegerter M A 1996 *Phys. Rev.* B **53** 6065
[6] Acioli L H, Guo J-T, de Araújo Cid B, Messaddeq Y and Aegerter M A 1997 *J. Lumin.* **72–74** 68
[7] Martín I R, Rodríguez V D, Lavín V and Rodríguez-Mendoza U R 1998 *J. Alloys Compounds* **275** 345
[8] Martín I R, Vélez P, Rodríguez V D, Rodríguez-Mendoza U R and Lavín V 1998 *Spectrosc. Acta* A **55** 935
[9] Judd B R 1992 *Phys. Rev.* **127** 750
[10] Ofelt G S 1962 *J. Chem. Phys.* **37** 511
[11] Weber M J, Varitimos T E and Matsinger B H 1973 *Phys. Rev.* B **8** 47
[12] Guéry C, Adam J L and Lucas J 1988 *J. Lumin.* **42** 181
[13] Yeh D C, Petrin R R, Sibley W A, Magigou V, Adam J L and Suscavage M J 1989 *Phys. Rev.* B **39** 80
[14] Tanabe S, Tamai K, Hirao K and Soga N 1993 *Phys. Rev.* B **47** 2507
[15] Lagriffoul C L, Moncorge R, Souriau J C, Borel C and Wyon C 1994 *J. Lumin.* **62** 157
[16] Jourbert M-F, Guy S, Linares C, Jacquier B and Adam J L 1995 *J. Non-Cryst. Solids* **184** 98
[17] Martín I R 1996 *PhD Thesis* Departamento de Física Fundamental y Experimental, Universidad de La Laguna
[18] Martín I R, Rodríguez V D, Alcalá R and Cases R 1993 *J. Non-Cryst. Solids* **161** 294
[19] Guy S, Bonner C L, Shepherd D P, Hanna D C, Tropper A C and Ferrand B 1998 *IEEEE J. Quantum Electron.* **34** 900
[20] Dyson J M, Jaffe S M, Eilers H, Jones M L, Dennis W M and Yen W M 1994 *J. Lumin.* **60/61** 668
[21] Guy S, Houbert M-F and Jacquier B 1998 *J. Alloys Compounds* **275–277** 186